Fully Convolutional Neural Network With GRU for 3D Braided Composite Material Flaw Detection

YONGMIN GUO[1,3], **ZHITAO XIAO**[2,3], **LEI GENG**[2,3], **JUN WU**[2,3], **FANG ZHANG**[2,3], **YANBEI LIU**[2,3], **AND WEN WANG**[2,3]

[1]School of Mechanical Engineering, Tianjin Polytechnic University, Tianjin 300387, China
[2]School of Electronics and Information Engineering, Tianjin Polytechnic University, Tianjin 300387, China
[3]Tianjin Key Laboratory of Optoelectronic Detection Technology and System, Tianjin Polytechnic University, Tianjin 300387, China

Corresponding author: Zhitao Xiao (xiaozhitao@tjpu.edu.cn)

ABSTRACT Automated ultrasonic signal classification systems are often utilized for the recognition of a large number of ultrasonic signals in engineering materials. Existing defect classification methods are mainly image-based and serve to extract features for various defects. In this paper, we propose a novel detection baseline model based on a fully convolution network (FCN) and gated recurrent unit (GRU) to classify ultrasonic signals from flawed 3D braided composite specimens with debonding defects. In the proposed algorithm, the proposed Gated Recurrent Unit Fully Convolutional Network (GRU-FCN) is used to extract temporal characteristics of ultrasonic signals; the GRU module is key to enhancing the performance of FCNs. Experimental results on an in-house dataset indicated that the proposed model performs very well against all baselines. We also developed a scheme to interpret the relationship between A-scan and C-scan images and a 3D depth model representation to visualize the location information of defects.

INDEX TERMS Ultrasonic signal classification, fully convolution networks, gated recurrent unit, 3D braided composite specimens, time series, C-scan images.

I. INTRODUCTION

Three-dimensional (3D) braided composites are broadly employed in a variety of industries [1] as per their advantages over conventional laminated composites, including high damage tolerance, through-thickness reinforcement, and anti-ablation capability. Internal defects must be accurately detected to improve the service life of materials. Ultrasonic methods are considered the most efficient method for non-destructive testing (NDT) in evaluating composite materials. The pulse-echo method is the most widely used ultrasonic method for thickness measurement and flaw location, which involves detecting echoes produced when an ultrasonic pulse is reflected from a discontinuity or interface in the tested specimen [2]. An ultrasonic transducer receives the reflected waves from defects and converts them to electrical signals. These signals, called A-scan signals containing information regarding the orientation, size, and type of the defects.

The associate editor coordinating the review of this manuscript and approving it for publication was Xiao-Yu Zhang.

The primary goal of the ultrasonic inspection of engineering materials is to detect, locate and classify internal defects as quickly and accurately as possible. The results of defect identification on A-scan signals usually depend on the knowledge and experience of operators, which is generally inefficient and can lead to false detections and missed inspections. Automatic signal classification systems are an attractive potential alternative for flaw detection [3]. Many previous researchers have developed such systems [4]–[7]. Computational intelligence methods based on SVM have been used to classify defects in CRFP [8]. Saraiva *et al.* [9] proposed a general framework that uses the ANN as a nonlinear classification tool. Simone *et al.* [10] presented two feature extraction techniques to classify ultrasonic nondestructive examination (NDE) signals in welded materials. Deep convolutional neural networks have been used to classify ultrasonic signals from CFRP specimens with voids and delaminations [11]. Other researchers have established multi-class defect classification methods based on the 1D local binary pattern algorithm for weld defects as well [12].
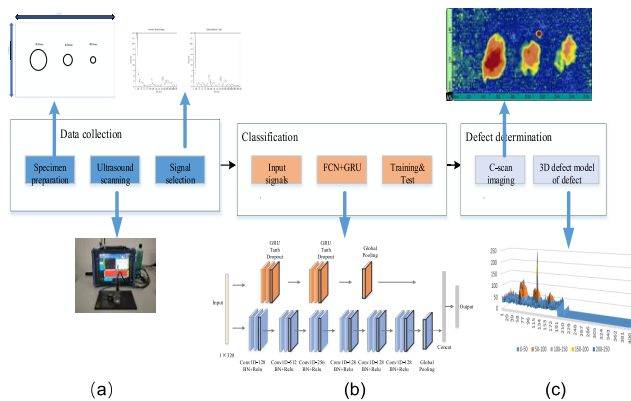
FIGURE 1. Flowchart of proposed approach. (a) Data collection process; (b) Signal classification including input signals, GRU-FCN architecture and training/testing; (c) Defect determination was performed by using C-scan imaging and 3D defect model.

Zhang et al. [13] attempted to resolve unbalance and inadequate training data issues using similar methods.

The above methods are mainly image-based generally inefficient, and are easily affected by image quality. Any classification problem using data that is registered in some type of order can be cast as a Time Series Classification (TSC) problem [14]. Time series have been applied ranging from electronic health records [15] and human recognition [16]–[17] to acoustic scene classification [18]. Ultrasonic signals can be viewed as time series, so we selected several baselines in this study for ultrasonic signals classification with deep learning architectures.

In this study, ultrasonic signals which were very similar to each other as-obtained from artificial inserts in a 3D braided composite plate were used to test a novel flaw detection technique. First, we produced a 3D braided plate with artificial defects and debonding. We then established an automated signal detection system based on FCN [19] and GRU [20] to process time series acquired via ultrasound transducer. In our previous task, Geng et al. [21] applied FCN and GRU to classify egg hatching activity. As mentioned above, the ultrasonic signals can be also viewed as time series, so several time series classification models were selected as baselines and 3,600 unique ultrasonic signals were tested as a dataset for classification. For more comprehensive defect information, we created a 3D depth model representation to characterize and localize defects. Below, we also propose a scheme to interpret the relationship between A-scan and C-scan images. Figure 1 represents a flowchart of our proposed approach.

A. CONTRIBUTIONS
The key contributions of this work are as follows.

1) A novel ultrasonic signal method for artificial defects detection in 3D braided composites is proposed. The ultrasonic signal of the specimen is used to classify defect versus non-defect areas. The results obtained using A-scan signals as the classification features are very accurate. Since the A-scan signals are a time series, they are easier to acquire and

collect than images, thus greatly enhancing the classification performance compared to image-based methods.

2) A baseline model based on the FCN module with a gated recurrent unit, the GRU-FCN, is the first attempt to detect ultrasonic signals from 3D braided composites. A GRU sub-module is used in the FCN model to obtain superior classification results.

3) We establish a scheme to interpret the relationship between A-scan and C-scan images and provide the defect information in 3D depth view.

B. RELATED WORKS
In recent years, various deep learning methods [22]–[24] have been applied to many classification tasks. Moreover, many recent researchers have pursued automated signal classification systems. Sambath et al. [4], for example, applied wavelet transform and an ANN classifier for defect detection and classification. Their ANN method has two layers with 25 nodes and 8 nodes, respectively, and reaches classification rate up to 94%. Meng et al. [11] used deep CNNs for training to classify ultrasonic defect signals from CFRP specimens where a linear SVM top layer is operated in the training process to perform the signal classification work. Veiga et al. [25] tested an ANN for ultrasonic signals acquired from weld beads by employing TOFD and pulse-echo techniques; four welding defects were classified by applying a supervised feed forward back propagation type neural network at a success rate of 77.5% for TOFD and 72.5% for the pulse echo technique. Cacciola et al. [8] proposed a feature extraction approach based on PCA and DWT. The SVM can be used as a heuristic pattern classifier trained on these features, the technique works well for UT signals from defective CFRP specimens. Munir et al. [26] used CNN and DNN on noisy ultrasonic signatures to increase classification performance of weldment defects. The CNN is the most robust structure for ultrasonic defect classification in terms of noisy signals. In this study, in an effort to enhance the effects of defect detection and defect characterization, an ultrasonic signal processing technique based on wavelet and wavelet packet transform was used.

The ultrasonic A-scan signal classification can be considered a TSC problem. Deep neural networks can be employed for TSC. The multi-scale convolutional neural network (MCNN) [27] incorporating feature classification and extraction in a single framework was proposed to provide superior feature representation by automatically extracting features at different scales and frequencies. However, its performance is strongly rely on the pre-processing applied to the dataset. FCN does not require any heavy data pre-processing. In this study, we attempted to detect ultrasonic signals as a time series for defect classification based on the FCNs by augmenting the FCN module with a GRU sub-module.

C. OUTLINE
Our work is structured as follows. The background works of the temporal convolutions and GRU are reviewed and

network architectures relevant to this study are detailed in Section 2. Our experimental procedure and results are discussed in Section 3. Section 4 characterizes and localizes 3D depth defect information. Section 5 contains a brief summary and conclusion.

II. METHODOLOGY

The proposed model is divided into two branches: FCNs and the GRU block. FCNs contain six temporal convolutions which typically served as the main feature extractors. The GRU block is comprised of two GRU layers that enhance the classification effect of FCNs. Ultrasonic signals as the time series are conveyed into both FCNs and the GRU block. Finally, the output features of FCNs and the GRU block are concatenated and classified via soft-max.

A. TEMPORAL CONVOLUTION NETWORKS

The temporal convolution network that receives the input is generally described as a time series, which is an effective learning model for the TSC problem [28]. According to Lea *et al.* [29], let us consider $X_t \in \mathbb{R}^{F_0}$ as an input feature vector of length F_0 for time step t, $t = 1, ..., T$. With different sequences, the time T may be different. Let T_l be the number of time steps in each step. The true action label for each frame is given by $y_t \in \{1, ..., C\}$, here C is the number of class labels.

Here, a set of 1D filters on each convolution layer were applied to see how the input signals evolve over the course of a given defect if there are L convolution layers. The filters for each layer are parameterized by tensor $W^{(L)} \in \mathbb{R}^{F_l \times d \times F_{l-1}}$, with corresponding bias vectors $b^{(l)} \in \mathbb{R}^{F_l}$, here $d, l \in \{1, ..., L\}$ represent the filter duration and the layer index, respectively. For the $l - th$ layer of the encoder, the $i - th$ component of the (unnormalized) activation $\hat{E}_{i,t}^{(l)} \in \mathbb{R}^{F_1}$ is a function of the incoming (normalized) signal $E^{(l-1)} \in \mathbb{R}^{F_{l-1} \times T_{l-1}}$ from the previous layer $\hat{E}_{i,t}^{(l)}$ can be computed as:

$$\hat{E}_{i,t}^{(l)} = f\left(b_i^{(l)} + \sum_{t'=1}^{d} \langle W_{i,t',.}^{(l)}, E_{.,t+d-t'}^{(l-1)} \rangle\right) \quad (1)$$

where $f(\cdot)$ denotes the Leaky Rectified Linear Unit [30].

B. GATED RECURRENT UNIT

Recently, Cho *et al.* [20] proposed the GRU to enable several recurrent units to adaptively acquire dependencies along different time scales. Similar to the LSTM unit, long dependency problems can also be solved by the GRU in recurrent neural networks (RNNs). The GRU has gating units that modulate the flow of information inside the unit, but does not have spate memory cells.

The activation function h_t^j is computed by:

$$h_t^j = \left(1 - z_t^j\right) h_{t-1}^j + z_t^j \tilde{h}_t^j \quad (2)$$

where h_{t-1}^j represents the previous activation; $\tilde{h}_t^j$ denotes the candidate activation. The extent to which the unit updates its

content or activation depends on an update gate z_t^j. We can calculate:

$$z_t^j = \sigma \left(W_z x_t + U_z h_{t-1}\right)^j \quad (3)$$

This procedure is similar to the LSTM unit, which can take a linear sum between the newly computed state and the existing state. However, the GRU exposes the whole state in each iteration.

The candidate activation $\tilde{h}_t^j$ is defined as follows [27]

$$\tilde{h}_t^j = tanh \left(W_{Xt} + U \left(r_t \odot h_{t-1}\right)\right)^j \quad (4)$$

Here, tanh is the hyperbolic tangent function, $\odot$ is the element-wise multiplication, and r_t refers to a set of reset gates.

The reset gate r_t^j is computed by:

$$r_t^j = \sigma \left(W_r x_t + U_r h_{t-1}\right)^j \quad (5)$$

C. NETWORK ARCHITECTURE

The proposed network is divided into two parts, FCNs and the GRU block. The FCNs and GRU block perceive the same ultrasonic signal input from two different perspectives. In the proposed network, FCNs comprise of temporal convolutions and act as the primary feature extractors. In the FCN block, each FCN is a convolution layer accompanied by a batch normalization [32] followed by a ReLU activation function. Batch normalization accelerates convergence, protects against divergence, and enhances the generalization capability.

The FCN module consists of six stacked temporal convolutional blocks with filter sizes of 128, 512, 256, 128, 128, and 128, respectively. The convolution operations are accomplished by six 1-D cores with the sizes $\{8, 5, 5, 3, 3, 3\}$. To prevent overfitting, we excluded any pooling operation. Finally, after the convolutional blocks, in order to minimize the number of weights needed, a global average pooling layer [31] was applied.

Simultaneously, an ultrasonic signal was conveyed into the GRU block to extract the temporal feature. The GRU module consists of two stacked basic GRU blocks. Each GRU block is a gated recurrent unit layer accompanied by dropout to prevent overfitting. Similarly to FCNs, after the final GRU block, a global pooling layer was applied. In the final step, the output of FCNs and the GRU module is concatenated and delivered to the soft-max layer. In the proposed architecture, the GRU module was applied to increase the performance of FCNs. The proposed network structure and neural network architectures, as shown in Figure 2 and Table 1, respectively.

III. EXPERIMENTS

A. SPECIMEN PREPARATION

Aerospace and automotive engineers often use 3D braided composites. The reinforced fibers in our specimens are T700-12K carbon fibers and the resin is LT-5080 A-OS vacuum impregnated with epoxy resin (Wells Advanced
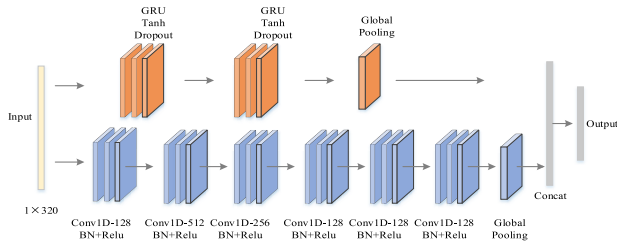
FIGURE 2. Network architecture. Table 1 shows more details.

TABLE 1. Neural network architectures.

Layer	0	1	2	3	4	5	6	7
Type	Input	TC	TC	TC	TC	TC	TC	GAP
Name	Input	Conv1d-1	Conv1d-2	Conv1d-3	Conv1d-4	Conv1d-5	Conv1d-6	GAP-1
Connect	-	0	1	2	3	4	5	6
Filter dim	-	8	5	5	3	3	3	-
Filter size	-	128	512	256	128	128	128	-
Activation	-	ReLU	ReLU	ReLU	ReLU	ReLU	ReLU	-
BN	-	Y	Y	Y	Y	Y	Y	-
Stride	-	N	N	N	N	N	N	-
Pad	-	valid	valid	valid	valid	valid	valid	-

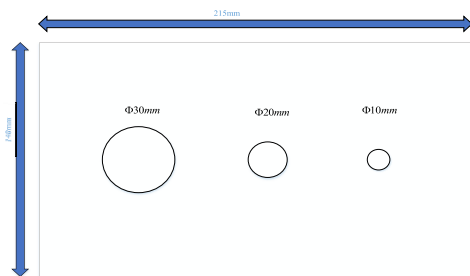| Layer	8	9	10	11	12	13	14
Type	GRU	GRU	GAP	Concat	FC	Softmax	Output
Name	GRU-1	GRU-1	GAP-2	Concat	Fc	Prob	Output
Connect to	0	8	9	7&10	11	12	12
Units	8	8	-	-	2	-	-
Activation	Tanh	Tanh	-	-	-	-	-
Dropout	0.5	0.5	-	-	-	-	-

FIGURE 3. Locations of debonding in 3D braided specimen.

Materials Co., Ltd.). Curing was performed in steps of 60°C for 3 h and post-curing at 80°C for 6 h.

A process was developed to produce a 3D braided composite with debonding defects. As shown in Figure 3, an artificial defective 3D 4-directional braided composite was fabricated with length of 215 mm and width of 140 mm with three debonding defects, then subjected to NDT measurements and signal acquisition.

B. EXPERIMENT DATA

We used an Olympus Omniscan MX2 to scan 3D braided composite structures for defects. For each 3D
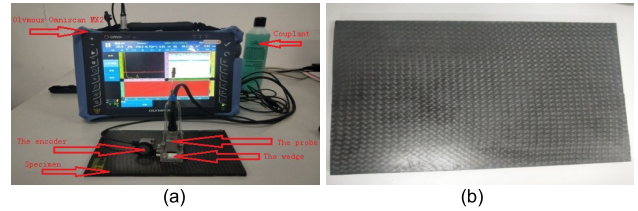

FIGURE 4. (a) Ultrasonic inspection system; (b) 3D braided composite specimen.
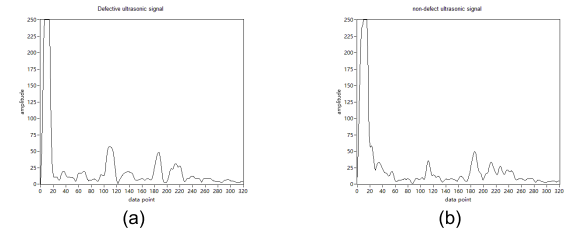

FIGURE 5. Original waveform of collected ultrasonic signal. Ultrasonic signal data processed by filtering and de-noising. (a) Non-defect ultrasonic signal; (b) Debonding defect signal.

braided composite, a 5MHz near-wall probe with 64 elements and a wedge (SNW1-OL-WP5) and encoder were used to record UT data (Olympus Corp., Tokyo, Japan) (Figure 4(a)). Experimental tests were performed on a 3D 4-directional rectangular flat with debonding defects, (Institute for Composites, Beijing 3D Braiding Co., Ltd.). The 3D flat braided specimen was made by a 4-step 1×1 method. The specimen size was 215×140×7 mm (Figure 4(b)).

In the study, we performed inspections on the 3D braided composite specimen with artificial debonding defects to test the proposed method experimentally. During ultrasonic signal acquisition, the specimen was set on the scanning stage and the probe moved it as probe water was coupled to the surface. A couplant was used to transmit the acoustic energy between the probe and the wedge. The A-scan signals were processed by filtering and de-noising on OmniPC 4.4 to enhance the classification accuracy. The ultrasonic signal was digitized at a simple length of 320.

The ultrasonic signals collected in the experiment are shown in Figure 5. The signals are very similar to each other as-obtained from the 3D braided composites. A dataset was constructed that consists of 3600 ultrasonic A-scan signals, 2100 of which show the absence of defects and 1500 with defects. The 3600 datasets were divided into training sets, test sets and validation sets accounting for 60%, 20% and 20% of the total, respectively.

C. EVALUATION METRICS

The ratio of negative and positive samples is imbalanced; there are many more non-defect signals than defect signals in our dataset. In addition, accuracy alone is insufficient to measure the classification results of the baseline models. Therefore, four different evaluation criteria including *Accuracy, Precision, Recall* and *F1 score* [33] were used to measure the proposed baseline comprehensively.

The confusion matrix, also called the "error matrix", a specific system including four parameters that measures the classification accuracy of a classifier. The four parameters are defined by the following formulas:

$$Accuracy = \frac{TP + TN}{TP + FN + TN + FN}$$

$$Precision = \frac{TP}{TP + FP}$$

$$Recall = \frac{TP}{TP + FN}$$

$$F1 = \frac{2TP}{2TP + FP + FN} \quad (6)$$

Among the above formulas, *TP*, *TN*, *FP* and *FN* are the numbers of true positive (predicted defect ultrasonic signals are actual defect ultrasonic signals), true negative (predicted non-defect ultrasonic signals are actual non-defect ultrasonic signals), false positive (predicted defect ultrasonic signals are actual non-defect ultrasonic signals) and false negative (predicted non-defect ultrasonic signals are actual defect ultrasonic signals) signals, respectively. *Accuracy* is the ratio of the number of samples correctly classified to the total number of samples. *Precision* is the ratio of the samples predicted to positive samples to actually positive samples. *Recall* is the proportion of correctly classified that should be classified. The F1-score is the harmonic average of the accuracy and recall rates.

To ensure a high-quality composite in an actual production scenario (Eq. (6)), *Recall* can be used to evaluate the ability of a baseline to identify positive samples. In other words, a higher *Recall* suggests a better capability of the baseline to recognize positive samples, which is great significance to analyze our experimental results. However, precision reflects the ability of a model to recognize negative samples. We expect an effective model to have higher recall than precision. The F1-score is a combination of accuracy and recall indicators; a higher F1-score indicates more robust classification ability.

D. BASELINES

In the study, to make the proposed model more competitive, several existing time series classification baseline models were selected.

1) ResNet [34], which inserts shortcut connections in each residual block to enable the gradients to flow directly through the bottom layers. However, the baseline RseNet is prone to overfitting due to the small size of the ultrasonic signal dataset and potential lack of sufficient variance to optimize the complex structures with deeper neural network systems. We explored the ResNet structure to classify ultrasonic signals for comparison. The ResNet consists of three residual blocks and the numbers of filters are {128, 256, 128} respectively. Each residual block consists of three convolution layers accompanied by a ReLu and a Batch normalization. After the final convolutional block, a global average pooling layer and a softmax layer are subsequently applied.

TABLE 2. Overall classification results for different enhancement modules.

Models	Modules	Acc	P	R	F1
FCN	--	0.9917	0.9836	**0.9833**	0.9916
LSTM-FCN	LSTM	0.9931	0.9863	**0.9861**	0.9930
CNN-FCN	CNN	0.9944	0.9890	**0.9889**	0.9944
GRU-FCN	**GRU**	**0.9972**	**0.9945**	**0.9944**	**0.9972**

Finally, these settings reuse of the FCN structure for fair comparison with the proposed model.

2) LSTM [35] is an extremely powerful sequence model that outperforms the general RNNs. Recently, RNNs with LSTM variants have been widely used to address the issues involved in sequence dataset [36]. However, convolution architectures with deep neural networks also obtain competitive performance for time series classification. Thus, a pure LSTM model was designed to compare their performance of the two frameworks (CNN, RNN) because we are interested to see which framework is better model for classifying our ultrasonic signals.

3) The GRU model outperforms the LSTM model on a set of tasks [37] although they have similar architectures. The GRU as another powerful RNN architecture. In this study, we sought to evaluate the performance of two closely recurrent units on our dataset.

We set similar hyperparameters for each baseline to compare baseline performance. Hyperparameters such as dropouts and learning rate for each baseline were chosen to adjust to optimize model performance. A random search was used to ensure well-performing baseline hyperparameters.

E. EXPERIMENT SETTINGS

The FCN module remained constant throughout our experiment and there was no data preprocessing. The initial batch size was 512 and the number of training epochs was kept constant at 300. After the final GRU layer, a dropout rate of 50% was applied to combat overfitting. All LSTM and GRU kernels were initialized by Xavier initialization [38]. The models were trained with Adam [38] at an initial learning rate of *1e-3* and a final learning rate of *1e-4*. The learning rate was reduced every 50 epochs by a factor of $1/\sqrt[3]{3}$ until the final learning rate was achieved.

The performance of our network was determined on a dataset, which consists of ultrasonic signals collected from a 3D braided composite specimen. To best represent the effectiveness of our baseline model, we designed three enhancement blocks (CNN, GRU, LSTM) to investigate their effects on the dataset. Table 2 and Figure 6 show the overall classification results with four metrics for different networks.

F. EFFECT OF DIFFERENT ENHANCEMENT MODULES

1) Our results indicate that CNN-FCN, GRU-FCN and LSTM-FCN are more effective than the sole FCN. The GRU-FCN clearly outperformed the other three methods as
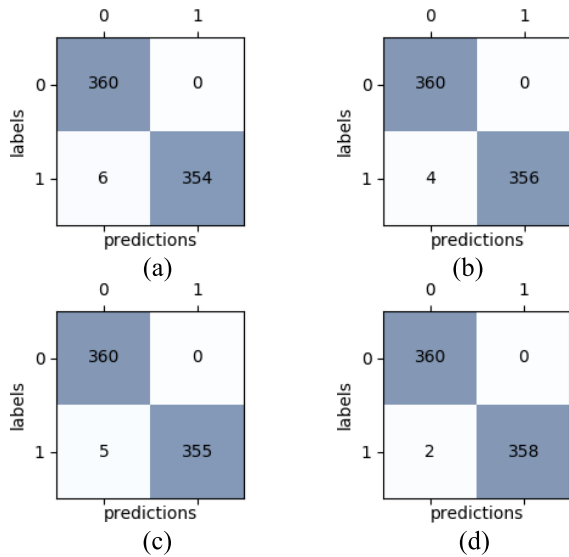
FIGURE 6. Confusion matrix of different models. (a) FCN, (b) CNN-FCN, (c) LSTM-FCN, (d) GRU-FCN.

per its higher generalization capability for classification on our database. This is because that GRU, CNN and LSTM blocks enable the FCN baseline to extract more temporal information of the ultrasonic signals. The addition of the LSTM, CNN, and GRU blocks improves the FCN classification performance of FCN.

2) The four evaluation metrics of the CNN-FCN are higher compared with those of the LSTM-FCN, which indicates that the convolutional module performs better ultrasonic classification than the LSTM module.

3) We also found that the GRU-FCN performed best classification performance on our ultrasonic signal database. Table 2 provides the recognition rate of the proposed method, where GRU-FCN achieves the highest *Accuracy, Precision, Recall* and *F1 score* among all the baselines we tested. Our goal here was to create a model with higher *Recall* than *Precision* for ultrasonic signals. Compared with the CNN-FCN, the recall rate of GRU-FCN increased by 0.55%. That suggests that the GRU-FCN model can effectively detect defect and non-defect ultrasonic signals and in practice and guarantee the quality of 3D braided composites.

G. OVERALL RESULTS

We used the benchmarks described above to test the performance of various models on our dataset (Table 3). The results suggest the following.

1) All of the FCN models with CNN, LSTM and GRU modules outperformed the other baselines by an order of magnitude. The baseline GRU-FCN achieved very competitive accuracy. The FCN models with the GRU blocks described here are suitable for classifying ultrasonic signals. The LSTM and GRU models performed very similarly. Similarly to the FCN, the ResNet model achieved favorable results on all four evaluation parameters. Convolutional-architecture

TABLE 3. Overall classification of different models on in-house dataset.

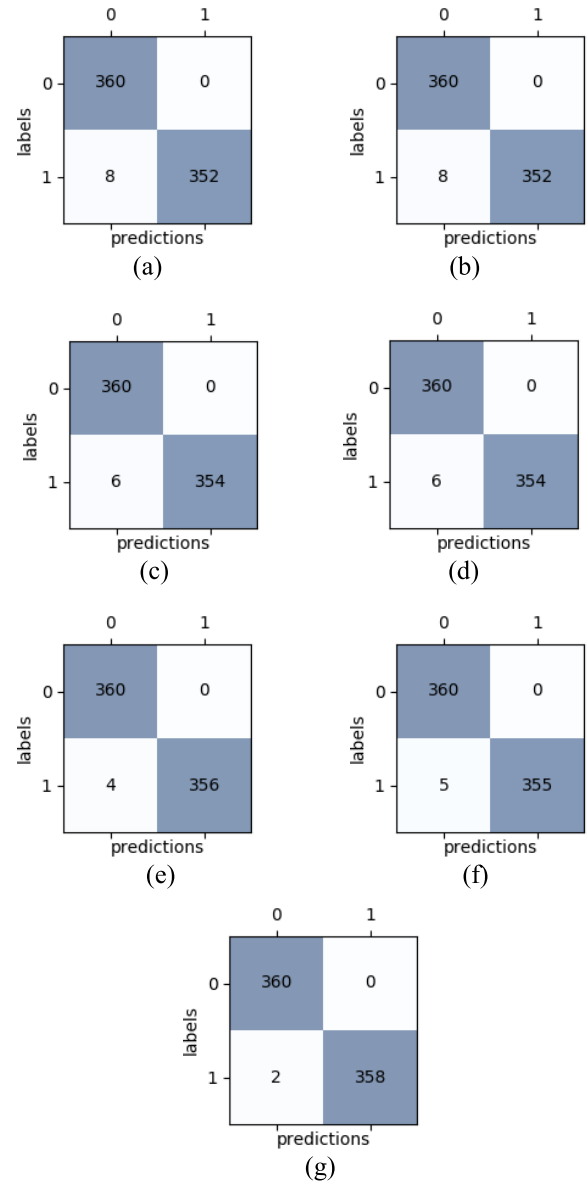| Models	ACC	P	**R**	F1
LSTM	0.9889	0.9783	**0.9778**	0.9888
GRU	0.9889	0.9783	**0.9778**	0.9888
ResNet	0.9917	0.9836	**0.9833**	0.9916
FCN	0.9917	0.9836	**0.9833**	0.9916
LSTM-FCN	0.9931	0.9890	**0.9861**	0.9930
CNN-FCN	0.9944	0.9890	**0.9889**	0.9944
GRU-FCN	**0.9972**	**0.9945**	**0.9944**	**0.9972**

FIGURE 7. Confusion matrix of different models. (a) LSTM, (b)GRU, (c) ResNet, (d) FCN, (e) CNN-FCN, (f) LSTM-FCN, (g) GRU-FCN.

networks appear to classify ultrasonic signals better than recurrent networks.

2) ResNet only outperformed the baselines of LSTM and GRU. In theory, ResNet should have achieved the best results due to its deepest network structure and greatest weight among the methods we tested. However, our dataset is very small and ResNet was more likely to overfit the data.
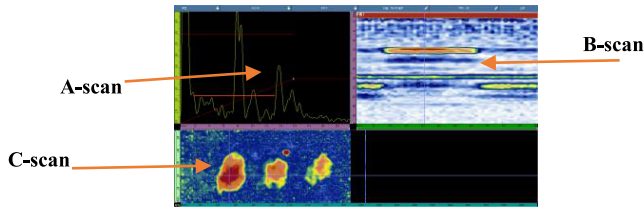
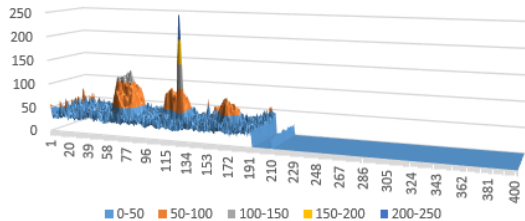**FIGURE 8.** Ultrasound signal representation.

FIGURE 9. Defect depth information in 3D visualization model.

IV. 3D REPRESENT FOR DEFECT DEPTH DETERMINATION

As discussed in this section, we established a scheme to characterize and localize the depth locations of defects.

A. ULTRASOUND SIGNAL REPRESENTATION

Ultrasonic signals can be represented as A-scan, B-scan and C-scan images for defect determination in 3D braided composites, as shown in Figure 8.

The A-scan displays the amplitude of the ultrasonic signals. A-scan signals are easy to collect and are commonly applied for processing in real world classification tasks, but it is difficult to make interpretations about the isolated A-scan signal without a reference signal recorded from a known defect-free area [39]. Thus, there is demand for a 2D representation based on B-scan and C-scan imagery. The B-scan image displays the depth of the potential defect and the C-scan image the top view of a specimen parallel to the scanned surface. Different color-codes of a defect in this case indicate the various depths at which the defects are located. A C-scan image including series of parallel A-scan signals is shown in Figure 8; where indeed the depth and size of the defect can be determined from the B-scan and C-scan images. The A-scan signals may continually vary in amplitude when the probe is moved on the surface of the specimen, suggesting that a C-scan image depends solely on the A-scan amplitude.

B. 3D DEPTH DEFECT VISUALIZATION

In our experiment, C-scan representations confirmed the presence of defects by showing clear plan views of the specimen parallel to the scanned surface but did not provide defect locations. We visualized defect locations through 3D depth model representations to account for this. The 3D depth representation described here was established to determine internal debonding defects, as shown in Figure 9. The corresponding A-scan, B-scan, and C-scan representations are shown in Figure 8.

V. CONCLUSION

In this study, we established an ultrasonic signal detection model using FCNs and a gated recurrent unit for defect detection in 3D braided composites. We classified the ultrasonic A-scan signals of 3D braided composites directly by using ultrasonic signals as a classification criterion. We first attempted to use the digital defect detector (Olympus Omniscan MX2) to collect ultrasonic A-scan signals of defective 3D braided composites with debonding defects. The proposed network structure for ultrasonic signal classification based on FCNs with GRU blocks was then used to extract ultrasonic signal features. Adding the GRU block allows the proposed model to adequately extract the temporal information of ultrasonic signals which discriminate defect classes consistently at very high classification accuracy.

We compared four evaluation metrics of six models. The results show that the proposed baseline model effectively classifies ultrasonic defect signals and achieves competitive performance on the same dataset compared to others. For defect determination, we also developed a scheme to interpret the relationship between A-scan and C-scan images. Finally, a 3D model representation was successfully used to characterize the depth of defects.

REFERENCES

[1] L. Tong, A. P. Mouritz, and M. K. Bannister, *3D Fibre-Reinforced Polymer Composite*. Amsterdam, The Netherlands: Elsevier, 2002, pp. 137–146. doi: 10.1016/B978-0-08-043938-9.X5012-1.

[2] ASM International, *Nondestructive Evaluation and Quality Control*, vol. 17, 9th ed. Cleveland, OH, USA: ASM International, 1992, p. 516.

[3] S. Iyer, S. K. Sinha, B. R. Tittmann, and M. K. Pedrick, "Ultrasonic signal processing methods for detection of defects in concrete pipes," *Autom. Construct*, vol. 22, pp. 135–148, Mar. 2012.

[4] S. Sambath, P. Nagaraj, and N. Selvakumar, "Automatic defect classification in ultrasonic NDT using artificial intelligence," *J. Nondestruct. Eval.*, vol. 30, no. 1, pp. 20–28, Mar. 2011.

[5] S.-J. Song, H.-J. Kim, and H. Cho, "Development of an intelligent system for ultrasonic flaw classification in weldments," *Nucl. Eng. Des.*, vol. 212, nos. 1–3, pp. 307–320, 2002.

[6] Y. Wang, "Wavelet transform based feature extraction for ultrasonic flaw signal classification," *J. Comput.*, vol. 9, no. 3, pp. 725–732, 2014.

[7] P. K. Wong, Z. Yang, C. M. Vong, and J. Zhong, "Real-time fault diagnosis for gas turbine generator systems using extreme learning machine," *Neurocomputing*, vol. 128, pp. 249–257, Mar. 2014.

[8] M. Cacciola, S. Calcagno, F. C. Morabito, and M. Versaci, "Computational intelligence aspects for defect classification in aeronautic composites by using ultrasonic pulses," *IEEE Trans. Ultrason., Ferroelectr., Freq. Control*, vol. 55, no. 4, pp. 870–878, Apr. 2008.

[9] F. de O. Saraiva, W. M. S. Bernardes, and E. N. Asada, "A framework for classification of non-linear loads in smart grids using artificial neural networks and multi-agent systems," *Neurocomputing*, vol. 170, pp. 328–338, Dec. 2015.

[10] G. Simone, F. Morabito, R. Polikar, P. Ramuhalli, L. Udpa, and S. Udpa, "Feature extraction techniques for ultrasonic signal classification," *Int. J. Appl. Electromagn. Mech.*, vol. 15, nos. 1–4, pp. 291–294, 2001.

[11] M. Meng, Y. J. Chua, E. Wouterson, and C. P. K. Ong, "Ultrasonic signal classification and imaging system for composite materials via deep convolutional neural networks," *Neurocomputing*, vol. 257, pp. 128–135, Sep. 2017.

[12] H. Hu, G. Peng, X. Wang, and Z. Zhou, "Weld defect classification using 1-D LBP feature extraction of ultrasonic signals," *Nondestruct. Test. Eval.*, vol. 33, no. 1, pp. 92–108, 2018.

[13] X.-Y. Zhang, H. Shi, X. Zhu, and P. Li, "Active semi-supervised learning based on self-expressive correlation with generative adversarial networks," *Neurocomputing*, vol. 345, pp. 103–113, Jun. 2019.

[14] J. C. B. Gamboa, "Deep learning for time-series analysis," 2017, *arXiv:1701.01887*. [Online]. Available: https://arxiv.org/abs/1701.01887

[15] A. Rajkomar *et al.*, "Scalable and accurate deep learning with electronic health records," *npj Digit. Med.*, vol. 1, no. 1, May 2018, Art. no. 18.

[16] H. F. Nweke, Y. W. Teh, M. A. Al-Garadi, and U. R. Alo, "Deep learning algorithms for human activity recognition using mobile and wearable sensor networks: State of the art and research challenges," *Expert Syst. Appl.*, vol. 105, pp. 233–261, Sep. 2018.

[17] J. Wang, Y. Chen, S. Hao, X. Peng, and L. Hu, "Deep learning for sensor-based activity recognition: A survey," *Pattern Recognit. Lett.*, vol. 119, pp. 3–11, Mar. 2019. doi: 10.1016/j.patrec.2018.02.010.

[18] T. L. Nwe, T. H. Dat, and B. Ma, "Convolutional neural network with multi-task learning scheme for acoustic scene classification," in *Proc. APSIPA ASC*, Kuala Lumpur, Malaysia, 2017, pp. 1347–1350.

[19] Z. Wang, W. Yan, and T. Oates, "Time series classification from scratch with deep neural networks: A strong baseline," in *Proc. IJCNN*, Anchorage, AK, USA, 2017, pp. 1578–1585.

[20] K. Cho, B. van Merrienboer, D. Bahdanau, and Y. Bengio, "On the properties of neural machine translation: Encoder-decoder approaches," 2014, *arXiv:1409.1259*. [Online]. Available: https://arxiv.org/abs/1409.1259

[21] L. Geng, H. Wang, Z. Xiao, F. Zhang, J. Wu, and Y. B. Liu, "Fully convolutional network with gated recurrent unit for hatching egg activity classification," *IEEE Access*, vol. 7, pp. 92378–92387, 2019.

[22] X.-Y. Zhang, S. Wang, and X. Yun, "Bidirectional active learning: A two-way exploration into unlabeled and labeled data set," *IEEE Trans. Neural Netw. Learn. Syst.*, vol. 26, no. 12, pp. 3034–3044, Dec. 2015.

[23] X.-Y. Zhang, S. Wang, X. Zhu, X. Yun, G. Wu, and Y. Wang, "Update vs. upgrade: Modeling with indeterminate multi-class active learning," *Neurocomputing*, vol. 162, pp. 163–170, Aug. 2015.

[24] X. Y. Zhang, H. Shi, C. Li, K. Zhang, X. B. Zhu, and L. X. Duan, "Learning transferable self-attentive representations for action recognition in untrimmed videos with weak supervision," in *Proc. AAAI*, Hawaii, HI, USA, 2019, pp. 9227–9234.

[25] J. Veiga, A. A. de Carvalho, I. C. da Silva, and J. M. A. Rebello, "The use of artificial neural network in the classification of pulse-echo and TOFD ultra-sonic signals," *J. Brazilian Soc. Mech. Sci. Eng.*, vol. 27, no. 4, pp. 394–398, 2005.

[26] N. Munir, H.-J. Kim, J. Park, S.-J. Song, and S.-S. Kang, "Convolutional neural network for ultrasonic weldment flaw classification in noisy conditions," *Ultrasonics*, vol. 94, pp. 74–81, Apr. 2019. doi: 10.1016/j.ultras.2018.12.001.

[27] Z. Cui, W. Chen, and Y. Chen, "Multi-scale convolutional neural networks for time series classification," 2016, *arXiv:1603.06995*. [Online]. Available: https://arxiv.org/abs/1603.06995

[28] G. Varol, I. Laptev, and C. Schmid, "Long-term temporal convolutions for action recognition," *IEEE Trans. Pattern Anal. Mach. Intell.*, vol. 40, no. 6, pp. 1510–1517, Jun. 2018.

[29] C. Lea, R. Vidal, A. Reiter, and G. D. Hager, "Temporal convolutional networks: A unified approach to action segmentation," in *Proc. 14th ECCV*, Amsterdam, The Netherlands, Aug. 2016, pp. 47–54.

[30] L. Trottier, P. Giguère, and B. Chaib-Draa, "Parametric exponential linear unit for deep convolutional neural networks," in *Proc. 16th ICMLA*, Cancún, Mexico, Dec. 2017, pp. 207–214.

[31] D. Bahdanau, K. Cho, and Y. Bengio, "Neural machine translation by jointly learning to align and translate," 2016, *arXiv:1409.0473*. [Online]. Available: https://arxiv.org/abs/1409.0473

[32] S. Ioffe and C. Szegedy, "Batch normalization: Accelerating deep network training by reducing internal covariate shift," 2015, *arXiv:1502.03167*. [Online]. Available: https://arxiv.org/abs/1502.03167?context=cs

[33] A. Özgür, L. Özgür, and T. Güngör, "Text categorization with class-based and corpus-based keyword selection," in *Proc. 20th Int. Symp. Comput. Inf. Sci.*, İstanbul, Turkey, 2005, pp. 606–615.

[34] K. He, X. Zhang, S. Ren, and J. Sun, "Deep residual learning for image recognition," in *Proc. CVPR*, Seattle, WA, USA, 2016, pp. 770–778.

[35] A. Graves, A.-R. Mohamed, and G. Hinton, "Speech recognition with deep recurrent neural networks," in *Proc. IEEE ICASSP*, Vancouver, BC, Canada, May 2013, pp. 6645–6649.

[36] A. Karpathy, J. Johnson, and L. Fei-Fei, "Visualizing and understanding recurrent networks," 2015, *arXiv:1506.02078*. [Online]. Available: https://arxiv.org/abs/1506.02078

[37] J. Chung, G. Gulcehre, K. Cho, and Y. Bengio, "Empirical evaluation of gated recurrent neural networks on sequence modeling," 2014, *arXiv:1412.3555*. [Online]. Available: https://arxiv.org/abs/1412.3555

[38] D. P. Kingma and J. Ba, "Adam: A method for stochastic optimization," 2014, *arXiv:1412.6980*. [Online]. Available: https://arxiv.org/abs/1412.6980

[39] S. Iyer, S. K. Sinha, M. K. Pedrick, and B. R. Tittmann, "Evaluation of ultrasonic inspection and imaging systems for concrete pipes," *Automat. Construct.*, vol. 22, pp. 149–164, Mar. 2012.

YONGMIN GUO is currently pursuing the Ph.D. degree with the School of Mechanical Engineering, Tianjin Polytechnic University, China. Her research interests include intelligent signal processing, nondestructive testing, image processing, and pattern recognition.

ZHITAO XIAO received the Ph.D. degree from the School of Electronics and Information Engineering, Tianjin University, in 2003. He is currently a Professor with the School of Electronics and Information Engineering, Tianjin Polytechnic University. His research interests include intelligent signal processing, image processing, and pattern recognition.

LEI GENG received the Ph.D. degree from the School of Precision Instrument and Optoelectronics Engineering, Tianjin University, in 2012. He is currently an Associate Professor with the School of Electronics and Information Engineering, Tianjin Polytechnic University. His research interests include image processing and pattern recognition, intelligent signal processing technology and systems, and DSP system research and development.
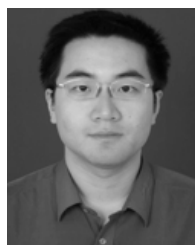
JUN WU received the Ph.D. degree from the School of Electronics and Information Engineering, Tianjin University, in 2007. He is currently an Associate Professor with the School of Electronics and Information Engineering, Tianjin Polytechnic University. His research interests include image processing and pattern recognition and artificial neural networks.

FANG ZHANG received the Ph.D. degree from the School of Precision Instrument and Optoelectronics Engineering, Tianjin University, in 2009. She is currently a Professor with the School of Electronics and Information Engineering, Tianjin Polytechnic University. Her research interests include image processing and pattern recognition and optical interference measurement technique.

WEN WANG received the master's degree in electronics and communication engineering from Tianjin Polytechnic University, in 2015, where she is currently an Assistant Lab Master with the School of Electronics and Information Engineering. Her major research interests include image processing and pattern recognition.

• • •

YANBEI LIU received the B.E. degree from the Zhengzhou University of Light Industry, Zhengzhou, China, in 2009, the M.E. degree from Tianjin Polytechnic University, Tianjin, China, in 2012, and the Ph.D. degree from Tianjin University, Tianjin, in 2017. He is currently a Lecturer with Tianjin Polytechnic University. His current research interests include machine learning, data mining, and computer vision.